

Thermally-fair Demand Response for District Heating and Cooling (DHC) Networks

Saptarshi Bhattacharya^{1*}, Vikas Chandan², Vijay Arya² and Koushik Kar¹

¹Rensselaer Polytechnic Institute, ²IBM Research, India

bhatts5@rpi.edu, vchanda4@in.ibm.com, vijay.arya@in.ibm.com,
koushik@ecse.rpi.edu

ABSTRACT

District heating and cooling networks (DHCs) are complex thermal grids wherein a centrally heated/cooled fluid is circulated through a network of pipes and heat exchangers to meet the heating/cooling needs of residential and commercial buildings. Several factors can hinder efficiencies and impartial distribution of energy among customers in these networks. These include varying levels of building insulation, distance of individual buildings from the central energy source, and thermal losses in network pipes. Moreover, shortage of energy at the central energy source and extreme weather conditions can exacerbate these issues, leading to differing levels of thermal comfort and customer disgruntlement in the long run.

In this paper, we propose and study a demand response scheme that attempts to ensure thermal fairness among end-use energy consumers in modern thermal grids. We develop optimization formulations based on thermodynamic models of DHCs, which determine optimal heat inflow/thermostat settings for individual buildings in order to achieve targeted thermal fairness across the network. Our experimental results using physics based models for DHC networks show that it is possible to achieve targeted thermal fairness based social welfare objectives in the DHC network by controlling network parameters such as mass flow rates of water to the consumer premises and the supply water temperature.

CCS Concepts

•Information Systems Applications → Miscellaneous;

Keywords

Thermal fairness, District Heating and Cooling (DHC) networks, Demand Response (DR)

1. INTRODUCTION

*The work was done during the author's internship at IBM Research, India.

Permission to make digital or hard copies of all or part of this work for personal or classroom use is granted without fee provided that copies are not made or distributed for profit or commercial advantage and that copies bear this notice and the full citation on the first page. Copyrights for components of this work owned by others than ACM must be honored. Abstracting with credit is permitted. To copy otherwise, or republish, to post on servers or to redistribute to lists, requires prior specific permission and/or a fee. Request permissions from permissions@acm.org.

e-Energy'16, June 21-24, 2016, Waterloo, ON, Canada

© 2016 ACM. ISBN 978-1-4503-4393-0/16/06...\$15.00

DOI: <http://dx.doi.org/10.1145/2934328.2934343>

In the backdrop of increasing renewable energy generation for catering to the global energy needs, District Heating and Cooling (DHC) networks are fast emerging as a major component of sustainable energy systems worldwide [14], [13], [16]. These DHC networks (also known as thermal grids) act as sustainable means of providing for the space heating and hot water requirements of buildings. They are particularly common in European countries (especially countries like Sweden, Finland and Denmark) where almost 62 million consumers are served through them, totaling about 12% of the entire population [1]. The main advantages of such networks lie in their ability to use waste heat from industrial processes, reduce emission levels, increase efficiency and flexibility of operation and integration with renewable energy systems.

Although sustainable to a large degree in general, an important limitation of these systems is the deficit of adequate energy available at the central energy source. For example, under extreme ambient conditions (very cold temperatures), if the energy available at the central energy source is not enough to sufficiently cater to the heating requirements of the entire network, then the network manager may be forced to procure energy from uneconomical fossil fuel based plants for satisfying the space heating requirements of all buildings in the network. Also, absence of centralized coordination and control of network parameters may often hinder fair energy distribution to end-use consumers within the thermal grid. This may lead to consumer disgruntlement in the long run. For example, uncoordinated operation may lead to lesser energy distribution in buildings located far away from the energy source leading to preferential treatment among consumers. Thus, it is imperative for grid managers to ensure fair distribution of available energy through centralized mechanisms so that the notion of *thermal fairness* is preserved within the network among the consumers.

The District Heating (DH) network which we model in this work has a centralized energy source that heats up the incoming cold water to be sent across a network of pipes to individual buildings, which then employ the hot water for their space heating purposes. We establish through numerical experiments that in scenarios of energy inadequacy, one possible way of avoiding (or reducing) the use of fossil fuel based energy is by implementing *demand-response (DR)* algorithms in the network. Through these DR algorithms, some buildings (consumers) are chosen to reduce their heating needs by some margin (thus becoming *DR facilitators*) and the conserved energy is effectively redistributed to other

buildings to achieve a greater degree of comfort (thus becoming *DR beneficiaries*). We then develop concrete optimization formulations to achieve targeted thermal fairness based social objectives through centralized control of network parameters such as mass flow rate of water to the buildings and the supply water temperature.

Note that the DR facilitators must be sufficiently compensated by the network manager/utility for accepting a margin of discomfort. The compensation structure and the economic aspects of the DR algorithm are an important part of the overall mechanism, but is outside the scope of this work. In this work, we mostly focus on the modeling aspects of a thermal grid and study appropriate DR frameworks in that network under various network objectives pertaining to thermal fairness. The rest of the paper is organized as follows. In Section 2, we describe the overall system model for a district heating network. We then empirically evaluate the potential for demand response in such a network in Section 3. In Section 4, we simplify the complex detailed system model in Section 2 by considering ideal conditions of operation and utilize the ideal model to develop the demand response optimization framework to achieve thermal fairness in Section 4.1. In Section 5, we extend our analysis to the case where the network is non-ideal with inherent thermal losses, and extend our optimization frameworks to such practical networks. We evaluate our algorithms through numerical studies in Section 6 and summarize our key findings along with future directions in Section 7.

1.1 Related work

Existing research has identified the need for controlling the system parameters within the thermal grids for optimizing social welfare objectives. For example, authors in [10] show that improvements in energy efficiency in a district heating network can be brought about by controlling mass flow rates of water to individual buildings. They also show that the topology of the network has an effect on the energy efficiency as well. Mass flow rate control for the optimal operation (minimized pumping loss and heat loss) of district heating networks has also been studied in [6]. Authors in [5] have developed optimal control strategies to minimize fossil fuel consumption in an integrated district heating system with availability of renewable energy sources like solar energy and wind energy. An approach for system cost minimization along with minimization of energy consumption for an entire year in district heating networks through a case study has been presented in [15]. Similar studies for modeling and optimization of operational cost for thermal grids have been proposed in [7]. A detailed modeling of a thermal grid along with a mass flow control methodology to achieve appreciable temperature cooling has been proposed in [9]. Several researchers have also identified the need for optimizing the supply temperature of water in district heating systems [3], [18], [11]. Authors in [3] propose a predictive control scheme using fuzzy Direct Matrix Control (DMC) for optimizing supply water temperature in district heating networks. Authors in [17] highlight the importance of properly selecting the control period for controlling the supply temperature of water. Authors in [2] discuss a methodology where mass flow rates and supply water temperature are optimized to minimize heat loss rate in thermal grids.

While the need for optimizing system cost, heat losses and supply water temperature within thermal grids has been

well established [6], [2], there is still a need for developing concrete demand response control strategies for optimizing social welfare objectives such as *thermal fairness*. Our key contribution in this work is that we consider the notion of thermal fairness and explicitly show how the centralized control of network parameters through demand response can lead to social welfare maximization within the thermal grid. Another contribution is that our physics based thermodynamic models for the DHC network are reasonably realistic and yet are amenable to analysis for gaining useful insights into the operation of the system. Additionally, our modeling allows us to frame our DR optimization problem as a simple convex optimization problem with linear constraints which is computationally viable for network managers (utilities).

2. MODELING THE DISTRICT HEATING NETWORK

We consider a district heating network as shown in Figure 1. Let $\mathcal{N}_b = \{1, 2, \dots, n\}$ represent the set of all buildings in the DH network. We assume a simple parallel topology to define the connectivity of the buildings in this network. Each building $i \in \mathcal{N}_b$ is assumed to have a thermal capacity C_i and an effective thermal insulation given by R_i . We assume that the energy distribution in buildings are subjected to thermal loss, which typically increases with their distances from the heat source. The heat source is assumed to be receiving cold return water at a temperature of T_R , and using the input power \dot{Q}_{in} is able to heat the water up to a supply temperature of T_S .

The heated water is networked through the connection of pipes to individual buildings as shown in Figure 1. During this transport, the thermal losses incurred along the way causes the effective supply temperature available (T_{MS}^i) at the mains (primary side) of the heat exchange circuit in building i to be less than T_S , i.e. $T_{MS}^i = T_S + w_i$ where $w_i < 0$ is the thermal loss (loss in temperature of supply water) incurred for building i . The effective incoming heat energy from the water is transferred to the house side (secondary side) of the heat exchange circuit which then has a supply temperature of T_{HS}^i . It must be noted that $T_{HS}^i \leq T_{MS}^i$. For our case, we assume that $T_{MS}^i - T_{HS}^i = \delta$, $\forall i \in \mathcal{N}_b$, where δ is the temperature differential between T_{MS}^i and T_{HS}^i . The hot water in the secondary side is now circulated through the radiators of the building (HVAC equipment) i to provide for space heating and ideally maintain the ambient zone temperature T_z^i of that building at a preferred set-point T_{sp}^i . The return cold water temperature in the secondary, i.e. T_{HR}^i , determines the return temperature in the mains i.e. T_{MR}^i . Subsequently the loss-adjusted return temperatures of the buildings i.e. the $T_R^i, \forall i \in \mathcal{N}_b$, determine the effective return temperature T_R of the water at the heat source.

2.1 Modeling of individual building thermodynamics

In this section, we attempt to capture the detailed thermodynamics of each individual building $i \in \mathcal{N}_b$, depending on several factors including its effective equivalent thermal parameters (R_i and C_i), its heat exchanger effectiveness ϵ_i , the respective supply and return temperatures in the primary and secondary of the heat exchanger circuit of the building, its radiator characteristics (including its thermal conductivity U_i and effective surface area A_i), and the ambi-

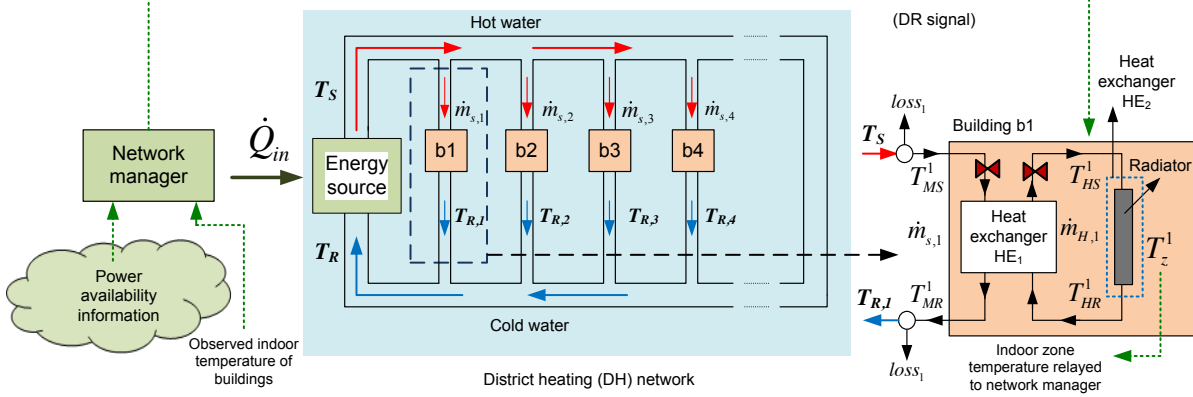


Figure 1: Schematic diagram of a district heating network where buildings are connected in parallel topology.

ent temperature T_∞ . Note that there are two heat exchange circuits: (a) HE_1 which captures heat exchange between the network pipes (primary/mains) and the house pipes (secondary), and (b) HE_2 which captures the heat exchange between the house pipes and the indoor house space through the radiator coils. We begin with the indoor zone temperature evolution. We assume that the indoor zone temperature (T_z^i) of a building i evolves according to,

$$\dot{T}_z^i = \frac{1}{R_i C_i} (T_\infty - T_z^i) + \frac{1}{C_i} \dot{Q}_a^i + \frac{1}{C_i} \dot{Q}_{HVAC}^i. \quad (1)$$

Here, \dot{Q}_a^i is the power generated by active elements (such as humans, lighting devices etc.) within building i and \dot{Q}_{HVAC}^i is the HVAC power available through the radiator of building i for indoor space heating. Note that

$$\dot{Q}_{HVAC}^i = \dot{m}_{H,i} C_p (T_{HS}^i - T_{HR}^i), \quad (2)$$

where $\dot{m}_{H,i}$, T_{HS}^i and T_{HR}^i are the mass flow rate, supply and return temperatures of the water in the secondary of HE_1 circuit respectively. C_p is the specific heat capacity of water. The effectiveness of heat exchanger in the HE_1 circuit is modeled according to,

$$\frac{T_{MS}^i - T_{MR}^i}{T_{MS}^i - T_{HR}^i} = \epsilon_i, \quad (3)$$

where ϵ_i is the heat exchanger effectiveness in building i . Note that $0 \leq \epsilon_i \leq 1$, $\forall i$. The radiator heat exchange dynamics in HE_2 circuit is governed by the equation,

$$\dot{Q}_{HVAC}^i = \dot{m}_{H,i} C_p (T_{HS}^i - T_{HR}^i) = U_i A_i (\Delta T_{eff}^i), \quad (4)$$

where ΔT_{eff}^i is the temperature difference between the radiator coils and the indoor ambient in building i . The ΔT_{eff}^i can be approximated as $\Delta T_{eff}^i \approx \left(\frac{T_{HS}^i + T_{HR}^i}{2} - T_z^i \right)$ for practical purposes. Finally, due to conservation of energy, we can also write,

$$\dot{m}_{s,i} C_p (T_{MS}^i - T_{MR}^i) = \dot{m}_{H,i} C_p (T_{HS}^i - T_{HR}^i) \quad (5)$$

where $\dot{m}_{s,i}$ is the mass flow rate of water in the primary/mains of HE_1 circuit.

2.2 Modeling of network thermodynamics

Assume that \dot{Q}_{in} is the total rate of heat energy available at the central source for district heating needs. From conservation of energy in the overall district heating network, we can write $\dot{Q}_{in} = \sum_{i \in \mathcal{N}_b} \dot{m}_{s,i} C_p (T_S - T_R^i)$. Noting that $\dot{Q}_{in} = \dot{M} C_p (T_S - T_R)$, where $\dot{M} = \sum_{i \in \mathcal{N}_b} \dot{m}_{s,i}$, we can express the return temperature of water (T_R) in the network as,

$$T_R = \frac{\sum_{i \in \mathcal{N}_b} \dot{m}_{s,i} T_R^i}{\sum_{i \in \mathcal{N}_b} \dot{m}_{s,i}} = \frac{\sum_{i \in \mathcal{N}_b} \dot{m}_{s,i} T_R^i}{\dot{M}}. \quad (6)$$

The network manager uses the available energy at central energy source \dot{Q}_{in} to heat up the cold return water (at T_R) to T_S as captured by the following equation.

$$T_S = \frac{\dot{Q}_{in}}{\dot{M} C_p} + T_R. \quad (7)$$

Note that thermal grid managers usually have an operating chart to determine the maximum T_S that can be employed given a certain T_∞ . Such considerations impose an upper bound $T_{S,sat}$ on the temperature to which supply water can be heated during operation.

3. MOTIVATION FOR DR IN A DHC NETWORK

In thermal grids, several factors may hinder the fair distribution of available energy among end-use consumers, as discussed in Section 1. In this section, we seek to evaluate the feasibility of ensuring fair distribution of energy among grid consumers by centrally controlling network parameters.

To this end, we consider a test district heating network of 10 buildings (small residential units) connected in a parallel topology as shown in Figure 1. Assume that the buildings have similar thermal capacities (i.e. C_i values) but have differing levels of thermal insulation parameters (R_i). The building nearest to the heat source is assumed to have the best insulation value, and insulation values are assumed to progressively decrease as buildings move farther away from central heat source. Note that in general buildings will have

arbitrary thermal parameters independent of location within the grid, but our assumptions relating to the nature of variation of building insulation parameters have been made for ease of exposition of our arguments. In general, however, our arguments hold true for any network.

We assume that the effective supply temperature available to any building i also depends upon its location with respect to the central energy source. Specifically, the effective supply temperature available at the mains of HE_1 circuit in any house, i.e. T_{MS}^i , is assumed to linearly decrease with increase in distance of that building from the central heat source. Thus the building farthest from heat source (which has worst insulation in this case) would have the least effective supply water temperature. The radiator characteristics of all buildings are assumed to be similar: $U_i A_i = 0.2$, $\forall i$, heat exchanger efficiency $\epsilon_i = 0.9 \forall i$, and the mass flow rate of water in the house side ($\dot{m}_{H,i}$) is assumed to be upper bounded by $\dot{m}_{ub} = 0.044 \text{ kg/sec}$ for all buildings (valve limits). We also assume that the preferred temperature setpoint in these buildings is 22°C . The subsequent experiments in this section are carried out over a 24 hour interval during which ambient temperature evolves as in Figure 5 (see Section 6). Note that for these experiments, we assume that each building i has a proportional controller controlling its $\dot{m}_{H,i}$ with an aim of reducing the temperature differential $T_{sp}^i - T_z^i$.

Under this setting, we evaluate the feasibility of demand response by centrally altering network parameters to achieve thermal fairness in the district heating network. Note that in general, the grid manager can control several parameters. These include the individual mass flow rates to buildings or the thermostat set points in buildings. In these experiments, we choose the *change in thermostat set point*, i.e. ΔT_{sp}^i as our demand response signal. This means that the effective set point of building i is $T_{sp}^i - \Delta T_{sp}^i$. A case of no demand response for building i is realized by setting $\Delta T_{sp}^i = 0$. In later sections, we also analyze the case where direct control of mass flow rates to buildings are used to optimize thermal fairness.

In this work, we are considering a district heating network in an energy constrained environment where the net thermal discomfort incurred over a time t is given as $d_i(t)$, where $d_i(t) = \max(0, T_{sp}^i - T_z^i(t))$. Intuitively, whenever the indoor space temperature of building i fails to reach its preferred set-point T_{sp}^i , the consumer in building i incurs discomfort. A method for quantifying the *social welfare* in the network in time period $[0, T]$ is through observation of the variance of the term D_i where $D_i = \int_{t \in [0, T]} d_i(t) dt$. A lower variance would indicate that the spread of the net discomfort faced by the buildings is narrow and thus buildings are subjected to similar discomfort levels in the network. A higher variance indicates the possibility of some buildings suffering more discomfort than others.

As a baseline reference, consider the case when there is no demand response, i.e. $\Delta T_{sp}^i = 0, \forall i$. This is when the variance of D_i is maximum: let this value be $\text{var}(D_i)_{\max}$. The normalized variance of D_i under a DR scenario is defined as $\text{var}(D_i)_{\text{norm}} = \frac{\text{var}(D_i)}{\text{var}(D_i)_{\max}}$, where $\text{var}(D_i)$ is the variance in D_i when there is demand response in the network. We define the *time-averaged total discomfort* in the entire DH network as $\left(\int_{t=0}^T \sum_{i \in \mathcal{N}_b} d_i(t) dt \right) / \left(\int_{t=0}^T dt \right)$. This gives us

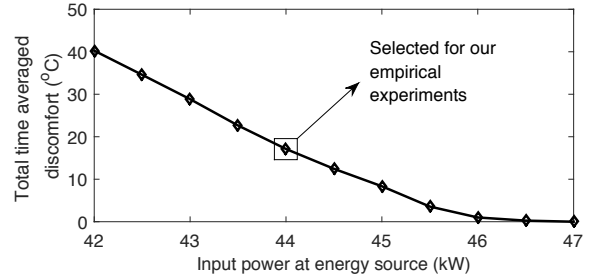


Figure 2: Effect of change in the the input source availability on the social welfare.

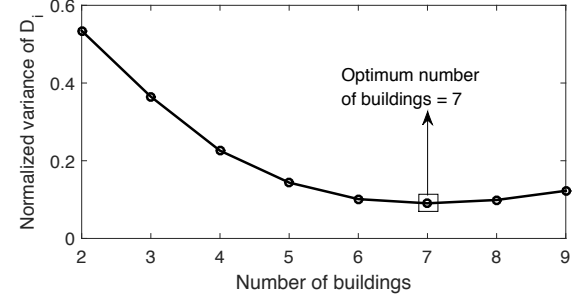


Figure 3: Effect of change in the number of buildings controlled for DR on social welfare.

a measure of the net system wide discomfort subject to a given ambient temperature profile and a given power availability at the input source. From Figure 2, we understand that the time-averaged total discomfort is dependent on the amount of power available at input source. In a practical scenario, the power availability is going to be variable across time slots, with underlying uncertainty. Here for the sake of study, we assume that the input power is constant during the 24 hour interval chosen for the study. We find that in a setting where $\dot{Q}_{in} = 44 \text{ kW}, \forall t \in [0, T]$, all buildings face some quantity of discomfort when there is no DR. Note that the choice of \dot{Q}_{in} is made entirely for illustration purposes; the experiment can be done under any other conditions of input power availability at the central heat source.

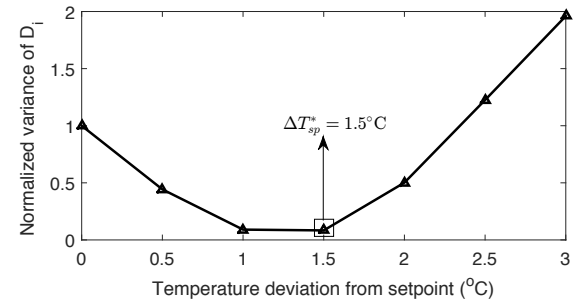


Figure 4: Effect of change in the T_{sp}^i of buildings controlled for DR on social welfare.

We now consider a varying number of buildings by setting the $\Delta T_{sp}^i = 1^\circ\text{C}$ for the buildings and evaluate the extent

of such control on the social welfare in the network. We observe from Figure 3 that the social welfare is optimized when 7 buildings are selected for demand response. Note that for imparting demand response, we select buildings in increasing order of their distances from the central heat source. In a subsequent study, we fix buildings 1 through 7 for imparting demand response by allowing change in their respective T_{sp}^i , and vary $\Delta T_{sp}^i, \forall i \in \{1, 2, \dots, 7\}$ in a range of values from 0°C to 3°C in intervals of 0.5°C. Note that in this study we change the set-point of all selected buildings by same amount. We observe from Figure 4 that under this setting, the maximum improvement in social welfare is observed when the set-point change is 1.5°C.

From the above experiments, we infer that demand response through centralized control of network parameters can indeed enhance thermal fairness within the network provided the number of buildings on which DR is applied and the extent to which DR is done is chosen carefully. Next, we will look to develop concrete algorithms through which optimal thermal fairness can be attained. We also demonstrate the distinction between such appropriate frameworks within ideal and non-ideal thermal grids.

4. ANALYSIS OF IDEAL DHC NETWORKS

In order to fully understand the energy distribution dynamics via fluid flow within an ideal district heating network, in this section, we make certain simplifying assumptions:

- The heat exchanger efficiency $\epsilon_i = 1 \forall i \in \mathcal{N}_b$.
- $\delta = 0, \forall i \in \mathcal{N}_b$, meaning $T_{MS}^i = T_{HS}^i, \forall i \in \mathcal{N}_b$.
- There are no thermal losses in the network, i.e. $T_{MS}^i = T_S, \forall i \in \mathcal{N}_b$.

From (3), since $\epsilon_i = 1$, we can write $T_{MR}^i = T_{HR}^i$. It also follows from our assumptions, that $(T_{MS}^i - T_{MR}^i) = (T_{HS}^i - T_{HR}^i) = (T_S - T_{MR}^i)$. Again, from (5), it follows that $\dot{m}_{H,i} = \dot{m}_{s,i}$. Let us denote $\dot{m}_{H,i} = \dot{m}_{s,i} = x_i$. Assuming $\dot{Q}_a^i = 0 \forall i \in \mathcal{N}_b$, and under steady state conditions when $\dot{T}_z = 0$, we can write directly from (1),

$$\frac{1}{R_i C_i} (T_\infty - T_z^i) + \frac{1}{C_i} \dot{m}_{H,i} C_p (T_{HS}^i - T_{HR}^i) = 0. \quad (8)$$

Applying our simplifying assumptions to (8), we can write,

$$\frac{1}{R_i C_i} (T_\infty - T_z^i) + \frac{1}{C_i} x_i C_p (T_S - T_{MR}^i) = 0. \quad (9)$$

Again, from (4) and our simplifying assumptions, we can write,

$$x_i C_p (T_S - T_{MR}^i) = U_i A_i \left(\frac{T_S + T_{MR}^i}{2} - T_z^i \right). \quad (10)$$

From (9) and (10), after rearranging the terms, we can write,

$$T_{MR}^i = \beta_i T_z^i - \alpha_i T_\infty - T_S, \quad (11)$$

where $\beta_i = \left(2 + \frac{2}{U_i A_i R_i} \right)$ and $\alpha_i = \frac{2}{U_i A_i R_i}$. Equation (11) allows us to express the steady state return temperature of the water from a building i in terms of the temperature of supply water T_S , the ambient temperature T_∞ and the

indoor zone temperature of building i i.e. T_z^i . Again from equations (9), (10) and (11) we can write,

$$x_i = \frac{\frac{1}{R_i} (T_z^i - T_\infty)}{C_p (2T_S - \beta_i T_z^i + \alpha_i T_\infty)}. \quad (12)$$

Equation (12) allows us to express the mass flow rate of building i under steady state operation as a function of the temperature of supply water T_S , the ambient temperature T_∞ and the indoor zone temperature of building i , T_z^i . Using the expressions for T_{MR}^i and x_i as obtained in (11) and (12) and the equations (6)-(7), and after simplification and rearrangement of terms, we can write,

$$\dot{Q}_{in} = \sum_{i \in \mathcal{N}_b} \frac{1}{R_i} (T_z^i - T_\infty). \quad (13)$$

From the above equation, we clearly see that under steady state operations in an ideal environment (such as the one assumed), the energy available at the central heat source is used to cater to the energy requirements for maintaining zone temperature in the buildings of the network.

4.1 Optimization framework for an ideal DHC network

In this section, we propose and analyze optimization formulations for demand response in the district heating network which are targeted to achieve social welfare based objectives. Note that in general, dynamic optimization formulations for an entire district heating network considering temperature transients, system losses and other network non-idealities over an extended duration of time (say 24 hours) tend to become computationally challenging owing to the large number of variables. Also, it becomes difficult to analytically examine the optimization formulation in such cases. Therefore, to circumvent these problems, we granularize the entire time duration into suitably small contiguous time windows. We then focus on optimization of mass flow rates in the ideal network within each time window when the ambient temperature is assumed to remain constant (say 1 hour) and considering steady state mode of operation. The overall dynamic control problem is therefore broken up into smaller subproblems, one for each time window.

In our framework, we consider that the control variable for invoking demand response in any building i is the mass flow rate x_i . In other words, given a certain ambient temperature T_∞ , we try to determine the optimal mass flow rate of water x_i^* that needs to be channelized to building i to achieve a network level social welfare objective. Another variable we want to determine is the optimal temperature T_S^* to which the supply water is to be heated.

4.1.1 Objective function

We discuss two types of objective functions for seeking thermal fairness within the district heating network.

1. **Minimize the maximum thermal discomfort of a consumer in the thermal grid:** In this case,

$$J_{fair} = \int_{t=0}^T \min \max_{i \in \mathcal{N}_b} (T_{sp}^i - T_z^i(t)), \quad (14)$$

where T_{sp}^i are the preferred temperature set point of consumers in building i . The notion of thermal discomfort in building i in this case, is given by the extent to

which the indoor zone temperature T_z^i is less than the preferred set point T_{sp}^i .

2. Maximize the overall utility in the thermal grid

Consider that consumer in building i has a utility function $U_i(T_z^i) = c_i - b_i(T_{sp}^i - T_z^i)^2$, where c_i and b_i are positive scalar constants. Such utility functions are common for thermostatic loads as seen in [12]. In such cases, a possible network objective for achieving thermal fairness would be,

$$J_{fair} = \int_{t=0}^T \max \sum_{i \in \mathcal{N}_b} U_i(T_z^i(t)). \quad (15)$$

Although we discuss the above two objectives in our work, it is worth noting that our proposed methodology can incorporate any other objective functions intended at optimizing thermal fairness in the network, as long as they satisfy certain convexity properties. As discussed before, we divide this optimization problem over $[0, T]$ into smaller subproblems, each on a smaller time window (say 1 hour). Next, we define the decision variables and associated optimization constraints for a single such small time window in the subsequent sections.

4.1.2 Decision variables

In our optimization framework, note that the decision variables are the temperature of the supply water and indoor steady state zone temperatures. Denote the decision variable vector as $\mathbf{T} = [T_S, T_z^1, T_z^2, \dots, T_z^N]$. An optimal point of operation corresponds to determining a set of optimal indoor zone temperatures for the N buildings i.e. $T_z^{i,*} \forall i \in \mathcal{N}_b$ and the optimal temperature of the supply water T_S^* . Note that the decision variable T_S does not appear in the objective functions we wish to analyze and hence needs to be determined separately as we will see subsequently. Also note that to achieve the optimal operating point, the requisite control variables in our formulation are the optimal mass flow rates x_i^* derived from (12), as a function of T_∞ , T_S^* and the corresponding $T_z^{i,*}$ values.

4.1.3 Optimization constraints

The first constraint for this optimization problem is the energy balance constraint as derived in equation (13). The next set of constraints deal with setting the upper and lower bounds for x_i , $\forall i \in \mathcal{N}_b$. Now, note that the mass flow rates in all buildings must be a non-negative value so $x_i \geq 0$, $\forall i \in \mathcal{N}_b$. For practical purposes, we can assume $(T_z^i - T_\infty) \geq 0$, $\forall i \in \mathcal{N}_b$. Therefore, using this information and (12), we observe that to make $x_i \geq 0$ for all buildings,

$$2T_S - \beta_i T_z^i + \alpha_i T_\infty \geq 0, \forall i \in \mathcal{N}_b. \quad (16)$$

Typically, mass flow rates of water in buildings will have an upper bound denoting the valve limits of the controller. Therefore,

$$x_i = \frac{\frac{1}{R_i}(T_z^i - T_\infty)}{C_p(2T_S - \beta_i T_z^i + \alpha_i T_\infty)} \leq x_i^{ub} \forall i \in \mathcal{N}_b. \quad (17)$$

The above set of inequalities can be simplified to be written as,

$$T_z^i \left(\frac{1}{R_i} + x_i^{ub} C_p \beta_i \right) - T_\infty \left(\frac{1}{R_i} + x_i^{ub} C_p \alpha_i \right) - 2x_i^{ub} C_p T_S \leq 0, \quad (18)$$

for all $i \in \mathcal{N}_b$. We also identify that in general, T_S should also be selected such that $T_S \leq T_{S,sat}$ (saturation constraint) where $T_{S,sat}$ is the maximum supply temperature at T_∞ ambient temperature, as obtained from the operating chart available to grid managers/operators. Let us denote the set \mathcal{D} be the set of all feasible vectors \mathbf{T} , such that (16) and (18) along with the saturation constraint $T_S \leq T_{S,sat}$ and energy balance constraint (13) hold. Therefore, the optimization problem for demand response in the district heating network can be written compactly as,

$$\min J_{fair}(\mathbf{T}), \quad (19)$$

$$s.t. \quad \mathbf{T} \in \mathcal{D}. \quad (20)$$

4.1.4 Selecting the optimal temperature of supply water (T_S^*)

Note that once the optimal steady state indoor zone temperature $T_z^{i,*}$ are determined from (19)-(20), the grid manager can rescale the optimal temperature to which the supply water needs to be heated i.e. T_S^* without affecting the $T_z^{i,*}$ values. It may be in the best interest of the grid manager to keep the T_S^* as low as possible since it minimizes thermal losses in the network and increases operational efficiency. To do this and yet maintain the respective $T_z^{i,*}$ and satisfy $0 \leq x_i^* \leq x_i^{ub}$, $\forall i \in \mathcal{N}_b$, the grid manager must observe the following:

- To ensure $x_i^* \geq 0$, $\forall i \in \mathcal{N}_b$, from (16), the optimal supply temperature must be such that,

$$T_S^* \geq \frac{1}{2} (\beta_i T_z^{i,*} - \alpha_i T_\infty) \quad \forall i \in \mathcal{N}_b. \quad (21)$$

- To ensure $x_i^* \leq x_i^{ub}$, from (17) the T_S^* has to be such that,

$$T_S^* \geq T_z^{i,*} \left(\frac{1}{2x_i^{ub} C_p R_i} + \frac{\beta_i}{2} \right) - T_\infty \left(\frac{1}{2x_i^{ub} C_p R_i} + \frac{\alpha_i}{2} \right), \quad (22)$$

for all $i \in \mathcal{N}_b$.

The grid manager then selects the minimum T_S^* that satisfies all the inequalities in (21) and (22). Selection of the T_S^* now allows determination of the optimum x_i^* for all buildings using equation (17) where $T_z^i = T_z^{i,*} \forall i \in \mathcal{N}_b$ and $T_S = T_S^*$. Thus the key observation is that for lossless networks, there may be a range over which the optimal supply water temperature T_S^* (the optimal x_i^* depend on the choice of T_S^*) can be heated to such that the optimal indoor temperatures $T_z^{i,*}$ (which are unique) may be attained. Equations (21)-(22) define the minimum T_S^* that can attain the optimal solution.

5. ANALYSIS OF PRACTICAL LOSSY DHC NETWORKS

In Section 4, we were able to understand the energy distribution dynamics of an ideal DHC network and use the knowledge to optimize key network parameters such as mass flow rates to buildings and the supply water temperature for realizing thermal fairness based social welfare objectives. However, in reality a DHC network will include several non-idealities which must be considered while trying to tune our network parameters with a view to realize similar social welfare objectives as in the last section.

Let us consider a lossy DHC network which has non-ideal heat exchangers in buildings, i.e. $\epsilon_i \leq 1$, $\forall i \in \mathcal{N}_b$ and $\delta > 0$. The thermal losses in the network typically depend (increase with) on the distance from the central energy source. Let w_i represent the thermal loss of the water supplied to building i . In other words, the effective supply water temperature at i is $T_{MS}^i = T_S + w_i$ where $w_i < 0$. Also, the effective return water temperature of building i at the source is $T_R^i = T_{MR}^i + w_i$. As in Section 4, we consider steady state scenario and express the steady state return temperature of water in the buildings in terms of the ambient temperature T_∞ , the supply temperature T_S , and the indoor zone temperature T_z^i . A similar line of analysis as in Section 4 enables us to write,

$$T_{MR}^i = \hat{\beta}_i T_z^i - \hat{\alpha}_i T_\infty - \hat{\gamma}_i T_{MS}^i + \epsilon_i \delta, \quad (23)$$

where $\hat{\beta}_i = 2\epsilon_i + \frac{2\epsilon_i}{U_i A_i R_i}$, $\hat{\alpha}_i = \frac{2\epsilon_i}{U_i A_i R_i}$ and $\hat{\gamma}_i = (2\epsilon_i - 1)$. The steady state primary side mass flow rates can be expressed as,

$$\dot{m}_{s,i} = \frac{\frac{1}{R_i}(T_z^i - T_\infty)}{C_p(2\epsilon_i T_{MS}^i - \hat{\beta}_i T_z^i + \hat{\alpha}_i T_\infty - \epsilon_i \delta)}. \quad (24)$$

Using these above quantities as obtained in (23) and (24) in (7), the steady state energy balance equation for a practical lossy network can be derived as,

$$\dot{Q}_{in} = \sum_{i \in \mathcal{N}_b} \frac{1}{R_i}(T_z^i - T_\infty) - 2 \sum_{i \in \mathcal{N}_b} \dot{m}_{s,i} C_p w_i. \quad (25)$$

Note that the second term in equation (25) accounts for the losses in the network. This was absent in (13) where an ideal and lossless DHC network was considered. Also note that all the steady state balance equations obtained in Section 4 can be retrieved from (23), (24) and (25) by putting $\epsilon_i = 1$, $\delta = 0$ and $w_i = 0$ for all buildings.

Remark: Note that for lossy networks, the presence of the mass flow rates $\dot{m}_{s,i}$ in the energy balance equation hinders the suitable rescaling of the supply water temperature (and hence the mass flow rates) and yet maintain the optimal steady state $T_z^{i,*}$ values as in the case of the lossless ideal network. Therefore, we put an additional constraint of upper bounding T_S by a suitable $T_{S,ub}$ within the optimization framework to directly compute system optimum \mathbf{T}^* under lossy cases using suitable mass flow rates $\dot{m}_{s,i}^*$, $\forall i \in \mathcal{N}_b$ in the primary circuit. We discuss this in details in the following subsection.

5.1 Optimization framework for practical DHC networks

The grid manager's objective is to control the mass flow rates of primary circuit (note that we cannot consider a single mass flow rate x_i as in the ideal network anymore due to inherent system non-idealities which leads to $\dot{m}_{s,i} \neq \dot{m}_{H,i}$ in general) to achieve social welfare objectives. The objective functions and the decision variables for optimization are exactly same as in Section 4.1. Let M_{ub} denote the upper bound on the mass flow rates. The first constraint is the energy balance equation as given in (25). The rest of the constraints in the lossy case can be summarized by the following set of equations,

$$2\epsilon_i T_{MS}^i - \hat{\beta}_i T_z^i + \hat{\alpha}_i T_\infty - \epsilon_i \delta \geq 0, \quad \forall i \in \mathcal{N}_b. \quad (26)$$

Inequalities in (26) lower bound the mass flow rates to be non-negative. The constraints relating to the upper bound are given as,

$$\lambda_1^i T_z^i - \lambda_2^i T_\infty - 2M_{ub}C_p\epsilon_i T_{MS}^i + M_{ub}C_p\epsilon_i \delta \leq 0, \quad \forall i \in \mathcal{N}_b, \quad (27)$$

where $\lambda_1^i = \left(\frac{1}{R_i} + M_{ub}\hat{\beta}_i C_p\right)$, $\lambda_2^i = \left(\frac{1}{R_i} + M_{ub}\hat{\alpha}_i C_p\right)$ are parametric constants of the system. The additional constraint on T_S can be written as,

$$T_S \leq T_{S,ub}. \quad (28)$$

In general, a good choice of $T_{S,ub}$ can be a few degrees lesser than the corresponding saturation temperature for supply water $T_{S,sat}$ at that respective T_∞ . After solving the above optimization problem, we can derive the optimal mass flow rates $\dot{m}_{s,i}^*$ for each building i in order to maintain set point temperature at $T_z^{i,*}$ and implicitly tune the steady state supply temperature to T_S^* . The above optimization problem is then solved for the subsequent time windows to determine the optimal mass flow rates and supply water temperature for the entire duration of DR.

6. EXPERIMENTAL RESULTS

In this section, we evaluate the optimization algorithms for demand response in the same network as was considered in Section 3. Note that the demand response mechanisms are studied over a period of 24 hours. The ambient temperature during this time is assumed to vary in accordance to the temperature of a typically extreme winter day in Lulea, Sweden; an area which caters to a sizable portion of local heating energy needs by district heating. The variation of the ambient temperature during this time is shown in Figure 5. We assume that the input power available for heating varies as shown in Figure 6. The preferred set points of all buildings throughout the optimization window is assumed to be 22°C .

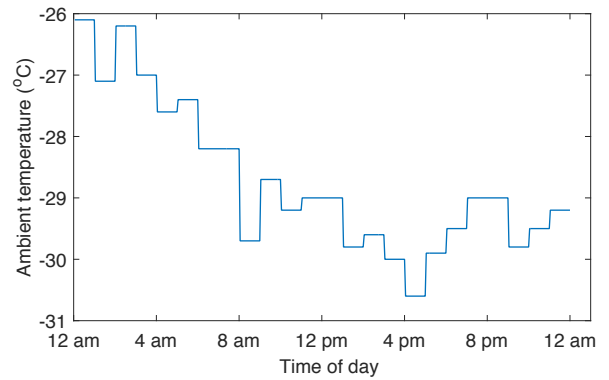


Figure 5: Ambient temperature variation during period of demand response.

The first experiment we conduct is to see how the network parameters and the individual zone temperatures evolve under conditions of no demand response. In such cases, the individual buildings are assumed to selfishly drive their indoor zone temperature towards their preferred set point by

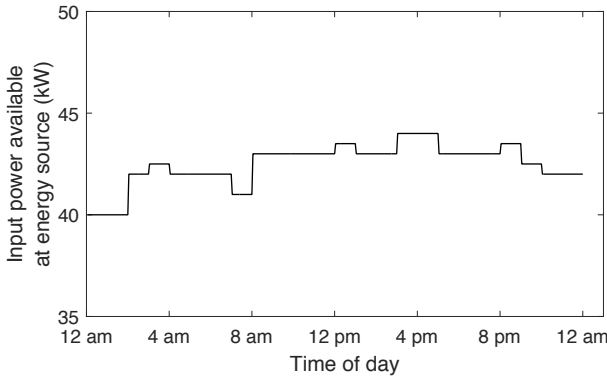


Figure 6: Variation of input power available for district heating at energy source during period of demand response.

controlling the secondary mass flow rates through a suitable proportional controller as was considered in Section 3. The secondary mass flow rate upper bound was considered to be 0.044 kg/sec as before. In this setting, we observe the evolution of the indoor zone temperature of the buildings. We then compare this with cases where demand response is initiated by the grid manager to effectively induce thermal fairness in the considered network. For better readability, in the remainder of this section, we only report the parameters of 5 of the 10 buildings (buildings numbers 1, 3, 5, 7 and 9) for studying the effects of demand response. Note that among these buildings, building 1 has the best thermal insulation and is subjected to least losses in the supply water temperature. The building insulation progressively decreases and temperature loss progressively increases with increase in building index. The thermal loss w_i (in $^{\circ}\text{C}$) in building i located y meters away from heat source is modeled by $w_i = -0.0027y + 0.84$. Building 1 is assumed to be located 320 meters from the energy source, and subsequent gaps between successive buildings are assumed to be 50 meters.

When there is no demand response, the indoor temperature profile of different buildings vary as shown in Figure 7. Clearly, buildings do not achieve desired set point since the \dot{Q}_{in} available (see Figure 6) during the studied window is insufficient for meeting their energy needs. We also observe that when there is no DR, building 1 is suffering the least discomfort and building 9 is suffering the maximum discomfort. This is owing to the lesser insulation in building 9 as compared to building 1 and greater thermal loss encountered by building 9 due to being located farther down the network from the central energy source. We now investigate the impact of demand response algorithms on the network. In our studies, motivated by the supply temperature curves in [4] we assume that $T_{S,sat} = 43 - 1.1T_{\infty}$. We also know that ideally the grid managers want to keep the supply temperature lower than the saturation to minimize losses in network. Hence, the optimization upper bound of T_S in our studies (which is also dependent on ambient temperature) is taken to be $T_{S,ub} = 36 - 1.1T_{\infty}$.

Also note that the demand response signals in our case are the mass flow rates in the primary circuit of the individual buildings as determined by the grid manager. Considering

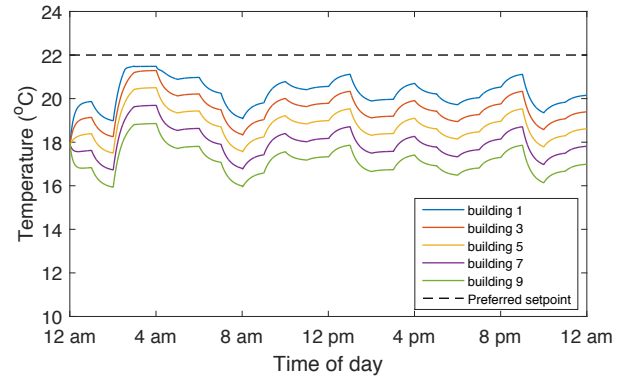


Figure 7: Variation of indoor zone temperature in buildings without any demand response.

the typical mass flow rates of water in radiator systems of residential buildings in different seasons [8], the upper bound on the primary mass flow rate to all buildings is selected as $M_{ub} = 0.044 \text{ kg/sec}$. In the first case we examine, the thermal fairness objective for the grid manager is to minimize the maximum discomfort faced by buildings, as defined by equation (14).

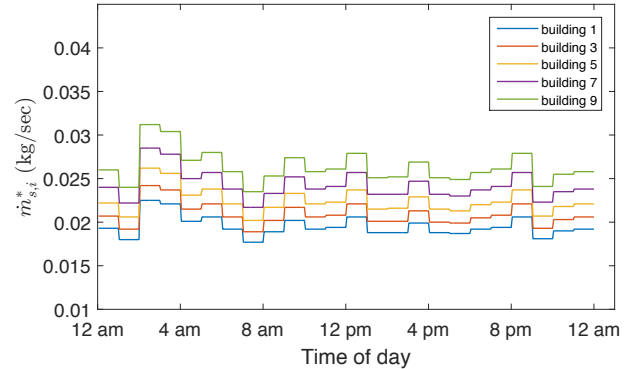


Figure 8: Variation of primary mass flow rates in buildings during period of demand response.

In Figure 8, we report the optimal mass flow rates $\dot{m}_{s,i}^*$ for each building i to realize the optimal set point temperature $T_z^{i,*}$. We observe that amount of water to be channeled to the building i increases with the increase in building index, i.e. grid manager channelizes more flow to less insulated buildings and buildings which face greater thermal loss in order to maximize the social welfare. In Figure 9, we observe that with these optimal mass flow rates, the indoor zone temperatures attained in the buildings are very close to each other (note that the temperature curves in Figure 9 are almost overlapping). Such network reconfiguration allows the consumers in the buildings to face similar levels of discomfort, hence optimizing the social welfare metric. We now investigate the effect of demand response on the supply water temperature.

We observe from Figure 10 that the optimal supply temperature of water T_S^* during the demand response is suit-

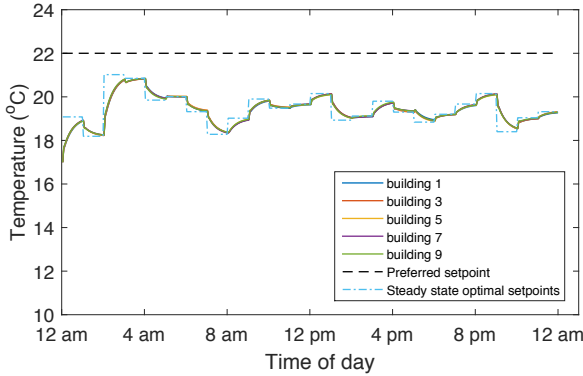


Figure 9: Variation of indoor zone temperature in buildings during period of demand response.

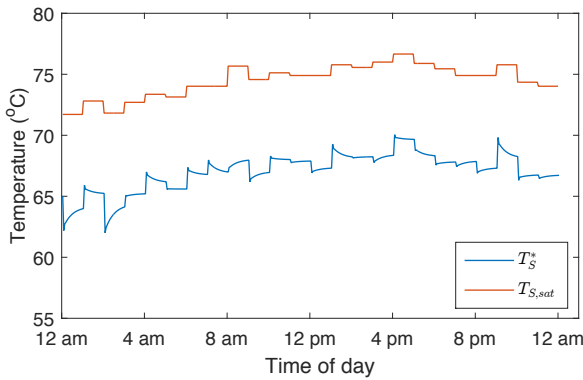


Figure 10: Variation of supply water temperature in the network during period of demand response.

ably maintained. In conjunction with the optimal mass flow rates, they control the indoor zone temperature in the buildings so as to achieve optimum thermal fairness. In order to quantify the improvement in thermal fairness across the entire network through demand response, we report the normalized discomforts, i.e. $D_{i,norm} = \frac{D_i}{\max_{i \in N_b} D_{i,no-DR}}$ (discomfort of building i is $D_i = \int_{t \in [0, T]} d_i(t) dt$) suffered by each of the buildings under two scenarios: (a) without demand response (when decentralized/greedy control of mass flow in buildings is allowed) and (b) with demand response.

We observe from Figure 11 that without any demand response, the discomfort suffered by buildings increase monotonically from building 1 to building 10. Through DR, the grid manager is seen to have effectively optimized the primary mass flow rates so that the overall time-averaged total discomfort in the network (as defined in Section 3) has decreased from 34.46°C to 25.88°C . As seen in Figure 11, with DR, the individual discomforts of buildings 4 to 10 have decreased. Therefore, these are classified as *DR beneficiaries*. However, discomforts in buildings 1 to 3 have slightly increased owing to DR. These buildings are thus classified as the *DR facilitators*. In practice, the grid manager has to provide incentives to the DR facilitators for facing greater discomfort. However, the design of such incentive mecha-

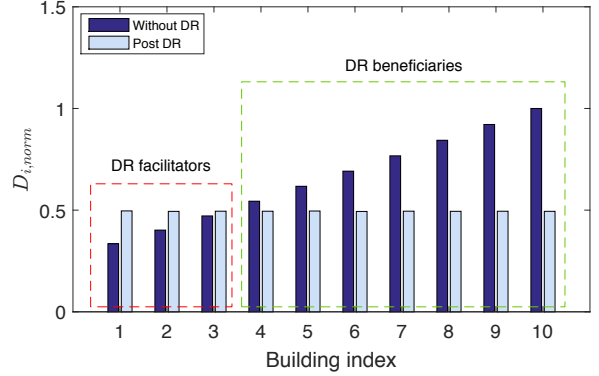


Figure 11: Discomforts faced by buildings before and after DR.

nisms require an independent investigation considering the grid manager's other economic considerations and hence we defer that to future work.

We repeat our experiment on the same test network under the same assumptions and settings with a different social welfare objective: to maximize overall utility in the network, as defined by (15). In this case, consumers in building i are assumed to have a concave utility function $U_i = c_i - b_i(T_{sp}^i - T_z^i)^2$. We assume $c_i = 10$ and $b_i = 0.05$ for all buildings. Under such a setting, the time-averaged total discomfort in the network was observed to come down from 34.46°C to 25.30°C . The optimal mass flow rates to the individual buildings, the resultant optimal supply temperature, the post DR indoor zone temperatures and the normalized discomfort of consumers in individual buildings before and after DR have been reported in Figures 12, 13, 14 and 15 respectively. Note that under this objective, the individual temperatures of the buildings are not as similar to each other as in the previous case. However, note that the reduction of time-averaged total discomfort in the network is slightly better under this setting. Thus, we infer that through various network objectives, we can achieve different levels of thermal fairness within the network by centralized control of network parameters.

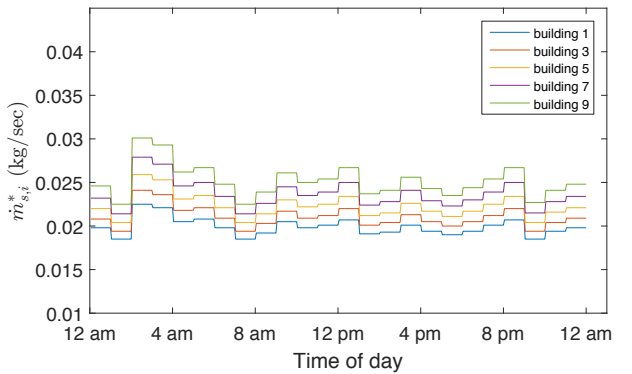


Figure 12: Variation of primary mass flow rates in buildings during period of demand response when optimization objective is utility maximization.

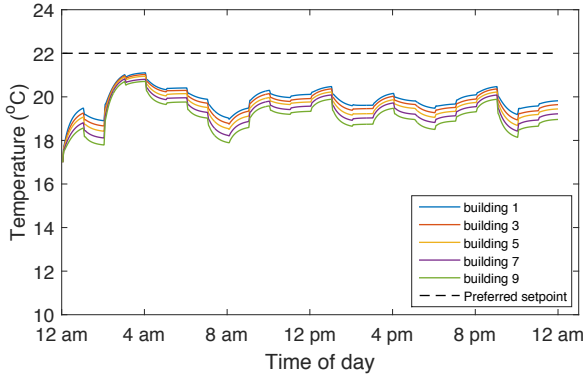


Figure 13: Variation of indoor zone temperature in buildings during period of demand response when optimization objective is utility maximization.

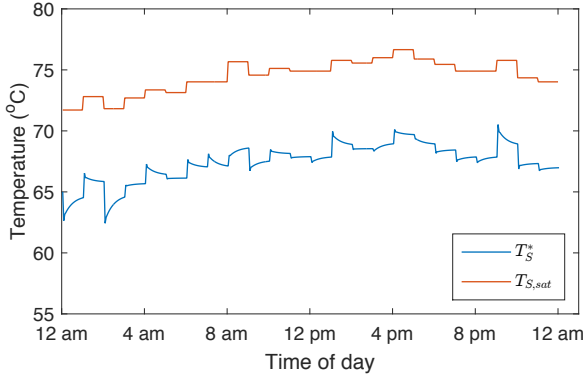


Figure 14: Variation of supply water temperature in the network during period of demand response when optimization objective is utility maximization.

7. DISCUSSION AND FUTURE WORK

In this work, we have presented a DR mechanism for thermal grids which optimizes network-wide thermal fairness based social welfare metrics. We modeled a thermal grid through detailed thermodynamics of the component buildings and demonstrated the scope of demand response in these networks to achieve thermal fairness. Through detailed analysis, we have proposed suitable optimization frameworks where network parameters such as mass flow of water to individual buildings are controlled in a centralized manner by the grid manager to realize the optimized temperatures in the buildings of the network. In this context, we have covered the scenarios of both an ideal network and a practical network (with non-idealities such as losses) and distinguished the differences between them and how that affects the DR mechanism. We demonstrate through experimental studies on a test network that such DR mechanisms are indeed able to significantly improve the selected social welfare metric when there is energy inadequacy in the central energy source. Finally, we note that proper incentive mechanisms must be developed to implement such DR mechanisms by the grid manager. This will require detailed investigation into economic considerations of the grid manager and is deferred to future work.

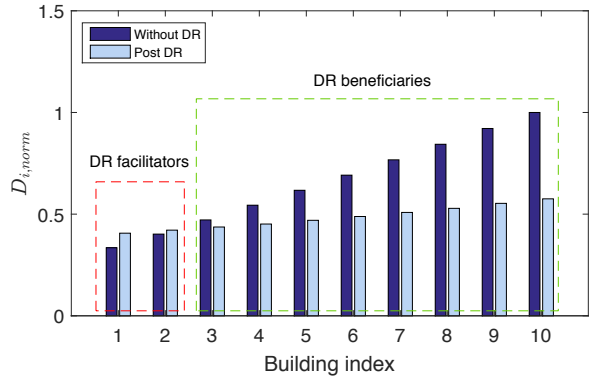


Figure 15: Discomforts faced by buildings before and after DR when optimization objective is utility maximization.

In this paper, while we have dealt with two objectives for improving thermal fairness, our framework can easily be extended to consider a broader set of social welfare metrics relating to thermal fairness. A dynamic optimization considering entire window of operation in a single shot may become computationally very resource intensive and hence, for large networks, may not be a viable solution to grid managers in the long run. Our optimization framework allows us to build the optimal set point of network operation over an extended duration by breaking it into smaller time slots, determining the optimum solution for that smaller time slot and repeating it to include the entire window. Thus it is amenable for use in larger networks hence making our DR mechanism easily scalable for implementation.

In this work, we have considered a parallel topology of the DHC network. Practical DHC networks may have different topologies like tree topology, ring topology, etc. Another point is that larger networks can also have multiple heat sources of different capacities within the network. We plan to extend our analysis to cover those cases as well and devise suitable DR mechanisms under such settings. Throughout this paper, we assume that the radiator characteristics, thermal insulation parameters of buildings and the thermal capacities of buildings are known to the grid manager. In practice, the thermal insulation parameters may change depending on the orientation of doors and windows within the buildings. Also, radiator performances may not always be equal to their rated performances. In light of such possibilities, a DR algorithm which is agnostic to the explicit knowledge of network parameters and can learn and adapt to the changing network parameters is desirable. We plan to investigate this aspect in our future work as well. In this context, with the advent of information and communication technologies, a fully data driven framework for modeling and subsequent optimization may also be a possibility, thus allowing us to bypass the use of physics based modeling altogether.

8. REFERENCES

- [1] Euroheat and power (DHC country by country survey 2013). www.dhcplus.eu/wp-content/uploads/2012/02/2010-report.pdf, 2013.

- [2] S.-J. Byun, H.-S. Park, S.-J. Yi, C.-H. Song, Y.-D. Choi, S.-H. Lee, and J.-K. Shin. Study on the optimal heat supply control algorithm for district heating distribution network in response to outdoor air temperature. *Energy*, 86:247–256, May 2015.
- [3] S. Grosswindhager, A. Voigt, and M. Kozek. Predictive control of district heating network using fuzzy dmc. In *2012 International Conference on Modelling, Identification and Control*, pages 241–246, June 2012.
- [4] J. Iturralde, M. Kuosa, T. Makila, M. Lampinen, and R. Lahdelma. Heat exchanger measurements in a mass flow controlled consumer substation connected to a ring network. *Applied Thermal Engineering*, 90:733–741, July 2015.
- [5] X. Jiang, Z. Jing, Y. Li, Q. Wu, and W. Tang. Modelling and operation optimization of an integrated energy based direct district water-heating system. *Energy*, 64:375–388, November 2013.
- [6] P. Jie, N. Zhu, and D. Li. Operation optimization of existing district heating systems. *Applied Thermal Engineering*, 78:278–288, January 2015.
- [7] Z. Jing, X. Jiang, Q. Wu, W. Tang, and B. Hua. Modelling and optimal operation of a small-scale integrated energy based district heating and cooling system. *Energy*, 73:399–415, July 2014.
- [8] T. Karlsson and A. Ragnarsson. Use of very low temperature geothermal water in radiator heating systems. In *World Geothermal Congress*,, pages 2193–2201, May 1995.
- [9] M. Kuosaa, M. Aalto, M. E. H. Assad, T. Makila, M. Lampinen, and R. Lahdelmaaa. Study of a district heating system with the ring network technologyand plate heat exchangers in a consumer substation. *Energy and Buildings*, 80:276–289, May 2014.
- [10] T. Laajalehto, M. Kuosa, T. Makila, M. Lampinen, and R. Lahdelma. Energy efficiency improvements utilising mass flow control and a ring topology in a district heating network. *Applied Thermal Engineering*, 69:86–95, April 2014.
- [11] P. Lauenburg and J. Wollerstran. Adaptive control of radiator systems for a lowest possible districtheating return temperature. *Energy and Buildings*, 72:132–140, December 2013.
- [12] N. Li, L. Chen, and S. H. Low. Optimal demand response based on utility maximization in power networks. In *2011 IEEE Power and Energy Society General Meeting*, pages 1–8, July 2011.
- [13] H. Lund, B. Moller, B. Mathiesen, and A. Dyrelund. The role of district heating in future renewable energy systems. *Energy*, 35:1381–1390, January 2010.
- [14] H. Lund, S. Werner, R. Wiltshire, S. Svendsen, J. E. Thorsen, F. Hvelplund, and B. V. Mathiesen. 4th generation district heating(4gdh) integrating smart thermal grids into future sustainable energy systems. *Energy*, 68:1–11, March 2014.
- [15] M. Pirouti, A. Bagdanavicius, J. Ekanayake, J. Wu, and N. Jenkins. Energy consumption and economic analyses of a district heating network. *Energy*, 57:149–159, March 2013.
- [16] B. Rezaie and M. A. Rosen. District heating and cooling: Review of technology and potential enhancements. *Applied Energy*, 93:2–10, 2012.
- [17] K. Steer, A. Wirth, and S. Halgamuge. Control period selection for improved operating performance in district heating networks. *Energy and Buildings*, 43:605–613, October 2010.
- [18] H. I. Tol and S. Svendsen. Operational planning of low-energy district heating systems connected to existing buildings. In *2nd International Conference on Renewable Energy: Generation and Applications*, 2012.